Hindawi Publishing Corporation
Advances in Materials Science and Engineering
Volume 2014, Article ID 730324, 10 pages
http://dx.doi.org/10.1155/2014/730324

Research Article

Evaluation of the Response of Posttensioned Steel Frames with Energy Dissipators Using Equivalent Single-Degree-of-Freedom Systems

J. Luz Rivera,[1] Arturo López-Barraza,[2] Sonia E. Ruiz,[2] and Alfredo Reyes-Salazar[1]

[1] *Facultad de Ingeniería, Universidad Autónoma de Sinaloa, Calzada de las Américas y Boulevard Universitarios S/N, Ciudad Universitaria, CP 80040, Culiacán Rosales, SIN, Mexico*
[2] *Coordinación de Mecánica Aplicada, Instituto de Ingeniería, Universidad Nacional Autónoma de México, Ciudad Universitaria, CP 04510, Coyoacán, Mexico*

Correspondence should be addressed to J. Luz Rivera; luz@uas.edu.mx

Received 25 March 2014; Revised 10 June 2014; Accepted 12 June 2014; Published 2 July 2014

Academic Editor: Jun Zhang

The hysteretic energy (E_H) dissipated in posttensioned steel frames (PTSF) with hysteretic dampers is calculated by using equivalent single-degree-of-freedom systems (ESDOFS), where the nonlinearity of both the steel bars (beam and columns) and the connections of the structural frame is separately considered. Five multi-degree-of-freedom (MDOFS) PTSF and their corresponding ESDOFS are studied under the action of 30 seismic motions recorded in soft ground, scaled in terms of the spectral pseudoacceleration evaluated at the fundamental period of the structures. Several simple mathematical expressions are proposed. The first expression is useful to calculate modifying factors (FM_{EH}) to relate E_H of the ESDOFS with that of the MDOFS; the second is to determine the interstory drift (γ) as a function of the seismic intensity. The third equation is to calculate the factor of the relative participation of the energy that the connections dissipate with respect to the total energy E_H and the fourth equation, which is function of the γ, is to obtain the distribution factors of E_H through the height of the structure. The methodology proposed can be used for the design or the structural revision of PTSF with dampers.

1. Introduction

Seismic design spectra corresponding to single-degree-of-freedom systems (SDOFS) are commonly used in structural engineering for the design of multi-degree-of-freedom structures (MDOFS). Seismic codes around the world normally specify design spectra corresponding to a certain return interval for this purpose; however, these spectra and the seismic design criteria recommended by the codes do not explicitly consider the hysteretic energy (E_H) dissipated by the structure which may be related to the cumulative structural damage. New tendencies in structural design are oriented to take into account E_H [1–4] particularly for structures subjected to long duration seismic ground motions like those occurring in the soft soil of the valley of Mexico. The energy concept for design purposes was first discussed by Housner [5]. Energy-based methodologies are aimed to provide the structures with an energy dissipating capacity that should be larger or equal than the expected energy demand [6].

There are approaches in the literature [7–9] for the seismic design of regular structural buildings that verify that the structure has the capability to control and accommodate simultaneously the maximum demands of (a) global ductility, (b) interstory drift, and (c) dissipated hysteretic energy. In particular, [9] makes use of (1) constant maximum ductility strength spectra and constant normalized dissipated hysteretic energy strength spectra and (2) transformation factors that take into account the differences between the response of MDOFS and ESDOFS. The approach is based on the understanding that spectra can be used to capture the global dynamic response of MDOFS; in other words, it is assumed

that through the use of spectra and appropriate ESDOFS to MDOFS transformation factors, the dynamic response of a regular steel building can be estimated for structural revision purposes.

The approaches mentioned in the paragraph above are applicable for the design of regular steel frames, but not for regular posttensioned steel frames (PTSF) with energy dissipating elements, like the structures analyzed here. In the present study, a transformation factor to estimate the seismic response of multi-degree-of-freedom with dissipating elements based on the response of ESDOFS is proposed. Furthermore, the criterion is extended to find the distribution of E_H through the height of the PTSF. The tools developed in the present study are useful to formulate design criteria of PTSF with dissipating elements that take into account the hysteretic energy dissipated by the structural elements.

The motivation behind the study of PTSF with dissipating elements is the increment of the use of the posttensioning technology in buildings around the world during recent years. Numerical and experimental results [10–15] show that buildings posttensioned connections are capable of achieving stiffness and stress comparable to those of traditional moment-resisting connections, as well as permitting the dissipation of seismic energy. This behavior can be achieved without the occurrence of inelastic deformations in beams and columns or residual structural drifts. This occurs because the connections with posttensioned elements and energy dissipating devices (PTED) include the high resistance of the posttensioned steel (which remains elastic during the seismic response), while the seismic dissipation of energy is confined to elements (i.e., steel angles) designed to develop large deformations in the inelastic range [16].

2. Model of a Single-Degree-of-Freedom System with PTED Connection

In this section, it is assumed that the global dissipated energy of multiple-degree-of-freedom PTSF with dissipating elements can be estimated from the response of ESDOFS, by means of adequate transformation factors.

To calculate the total energy dissipated by the structure, an ESDOFS that separately takes into account the nonlinearity of (1) the structural frame (beams and columns) and (2) the connections is proposed. The model used to represent the structure and the beam-column connection is formed by a simple oscillator with two parallel springs plus a dashpot, as shown in Figure 1. The contribution of each spring is independently considered because the hysteretic behavior of each element has different behavior under cyclic loads.

The linear equation of motion of the model under seismic load is

$$m\ddot{x} + c\dot{x} + \left(k_{\text{str}} + k_c\right) x = -m\ddot{x}_g, \tag{1}$$

where $\ddot{x}$, $\dot{x}$, and x are the acceleration, velocity, and displacement of the main system, respectively, m is the mass, c is the damping, and k_{str} and k_c are the stiffness of the structural system (beams and columns) and of the connection, respectively.

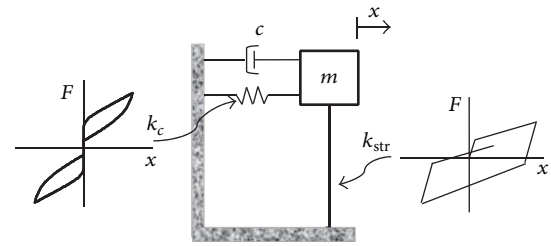

Figure 1: Equivalent single-degree-of-freedom system.

The nonlinear equation corresponding to the combined system is

$$m\ddot{x} + c\dot{x} + k_{\text{str}}\alpha_2 x + \left(1 - \alpha_2\right) k_{\text{str}} z + F = -m\ddot{x}_g. \tag{2}$$

The terms $k_{\text{str}}\alpha_2 x + (1 - \alpha_2)k_{\text{str}} z$ represent the restoring force of the main structural system; the first and second terms represent nonlinear nonhysteretic and nonlinear hysteretic components, respectively, of the structural restoring force; $\alpha_2 = k_{\text{str}(p)}/k_{\text{str}}$ is the ratio between the postyielding and the initial stiffness of the main structural system (elastic behavior); and z represents the hysteretic component having units of displacement [17].

The term F in (2) describes the flag-shaped hysteretic behavior of the connection in terms of the force-displacement relationship, and it is given by (3) and (4) for the unloading and loading cycles, respectively [18, 19]:

$$F = F_d + \frac{\left(k_c + k_{c(p)}\right) x}{\left[1 + \left|(k_c - k_{c(p)})x/F_0\right|^N\right]^{1/N}} + k_{c(p)} x, \tag{3}$$

$$F = F_a - \frac{\left(k_c + k_{c(p)}\right)\left(x_a - x\right)}{\left[1 + \left|(k_c - k_{c(p)})(x_a - x)/\beta F_0\right|^N\right]^{1/N}} - k_{c(p)}\left(x_a - x\right), \tag{4}$$

where $k_{c(p)}$ is the postyielding stiffness of the connection, N defines the transition zone from elastic to inelastic behavior, β defines the width of the flag, F_d is the decompressing force (exactly when the connection opens), $F_0 = F_y - F_d$ (F_y is the yield force in the PTSF), and x_a and F_a are the maximum displacement and maximum force reached in each load cycle, respectively. Equation (3) is used for either positive or negative load cycles, while (4) is for unloading. Figure 2 shows a hysteretic cycle of the semirigid posttensioned connection; the parameters previously mentioned are indicated in the figure, as well as the parameter F_c which is the force when the connection closes. Parameter values of (3) and (4) were obtained by means of incremental static analyses (push-over) and are given in Table 1, where F4 represents a 4-story frame; this notation is also applied for the other models with number of stories ranging from 6 to 14.

Table 1: Parameters used in (3) and (4).

Frame	F_0 (kN)	F_d (kN)	β	N	k_c (kN/m)	$k_{c(p)}$ (kN/m)
F4	122.6	578.8	2	2	17330	1881
F6	313.9	932.0	2	2	18556	2040
F8	348.3	932.0	2	2	18150	2044
F10	480.7	1128.2	2	2	18937	2202
F14	282.5	981.0	2	2	12422	1609

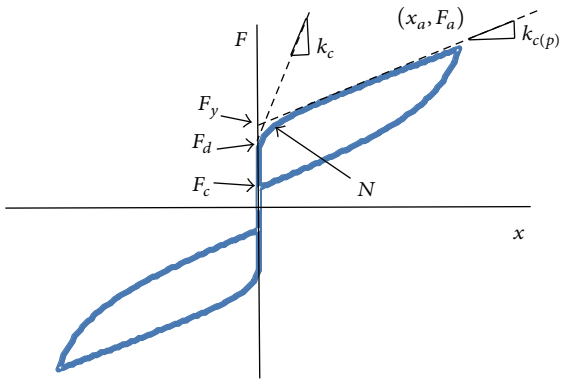

Figure 2: Hysteretic behaviour of the connection.

Dividing (2) by m and expressing it by the following system of differential equations, the following is obtained:

$$\ddot{x} = -\frac{c}{m}\dot{x} - \frac{k_{\text{str}}}{m}\alpha_2 x - (1-\alpha_2)\frac{k_{\text{str}}}{m}z - \frac{F}{m} - \ddot{x}_g,$$
$$\dot{z} = \frac{\alpha_3\dot{x} - \upsilon\left(\alpha_4 z\,|\dot{x}|\,|z|^{\alpha_6-1} + \alpha_5\dot{x}|z|^{\alpha_6}\right)}{\eta}, \quad (5)$$

where $\alpha_3, \alpha_4, \alpha_5$, and α_6 are the parameters of the model proposed by Bouc [20] and modified by Baber and Wen [21], that control the amplitude, the shape of the hysteretic cycle, and the smoothness of the transition from the elastic to the inelastic zone; η and υ are parameters that control the deterioration of both stiffness and strength. In this study, no structural deterioration was considered. The parameter values of α_4 and α_5 for steel structures are equal to [22] $\alpha_4 = \alpha_5 = (1/2\upsilon)(k_{\text{str}}/F_{\text{str}})^{\alpha_6}$, where F_{str} represents the yield force of the structural system and k_{str} is the structural stiffness. The values for α_3 and for α_6 were assumed to be equal to 1 and 15, respectively.

By introducing the variables $y_1 = x; y_2 = \dot{x}$; and $y_3 = z$, the system of (5) can be written as the following system of first-order differential equations:

$$\dot{y}_1 = y_2,$$
$$\dot{y}_2 = -\frac{c}{m}y_2 - \frac{k_{\text{str}}}{m}\alpha_2 y_1 - (1-\alpha_2)\frac{k_{\text{str}}}{m}y_3 - \frac{F}{m} - \ddot{x}_g, \quad (6)$$
$$\dot{y}_3 = \frac{\alpha_3 y_2 - \upsilon\left(\alpha_4 y_3\,|y_2|\,|y_3|^{\alpha_6-1} + \alpha_5 y_2|y_3|^{\alpha_6}\right)}{\eta}.$$

By solving (6), the displacement, velocity, and acceleration of the main structure are calculated, as well as the hysteresis cycles of both the main system and the PTED connections. The corresponding E_H is obtained by calculating the area enclosed by the hysteretic curves. The sum of the energies of both the main system and the connections is the total energy that the combined system dissipates.

3. Algorithm for Obtaining the Transformation Factors between ESDOFS and MDOSFS

The steps proposed to calculate the transformation factors between the response of the ESDOFS and MDOFS are as follows.

(1) The dynamic characteristics of the ESDOFS are assumed to be equal to those of the MDOFS to be analyzed. The properties are as follows: the fundamental structural vibration period (T_1), the damping (c), the yield force of the main system (F_{str}), and the elastic and plastic stiffness of the main system and connections (k_{str}, $k_{\text{str}(p)}k_c$, $yk_{c(p)}$). The values of both F_{str} and stiffness are obtained by means of "push-over," as was mentioned in Section 2, for the MDOFS with and without PTED connections.

(2) The mass of the ESDOFS is calculated as $m = k_T T_1^2/(2\pi)^2$, where $k_T = k_{\text{str}} + k_c$.

(3) The yield displacement of the structural system is obtained by the ratio $d_{\text{str}} = F_{\text{str}}/k_{\text{str}}$.

(4) The parameter α_2 corresponding to the hysteretic model of the structure is calculated.

(5) The earthquakes recorded in soft ground of Mexico City are scaled [23]. More details about the scaling criterion are given later.

(6) The response of the combined ESDOFS is calculated by using a "step-by-step" time history method (the fourth-order Runge-Kutta method was used herein). The dissipated hysteretic energy, the maximum restoring force, and the maximum displacement of the system are obtained by solving (6).

(7) The response of the MDOFS with dissipating elements is calculated by means of a "step-by-step" dynamic analysis in time domain.

(8) Once the responses of the MDOFS and their corresponding ESDOFS are calculated, the transformation

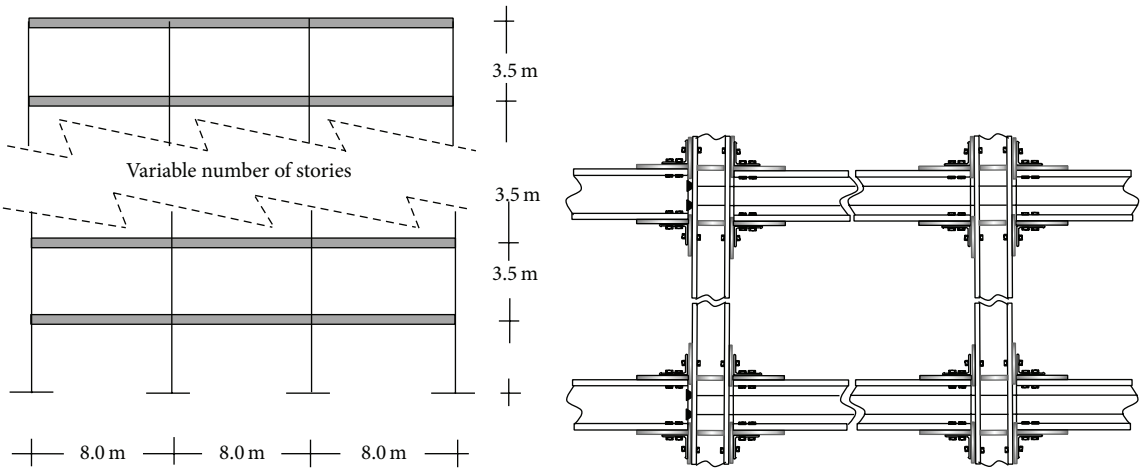

(a) Dimension of the frames (b) Angles and posttensioned strands

Figure 3: Geometrical characteristics of the frames with PTED connections.

factors that relate the responses of both structural systems are obtained as follows:

$$FM_{EH} = \frac{R_{\text{MDOFS}}}{R_{\text{ESDOFS}}}, \tag{7}$$

where FM_{EH} is the transformation factor of the response parameter of the ESDOFS to obtain that of the MDOFS and R is the response parameter. Dissipated hysteretic energy was the parameter selected in this study, but it could be any other parameter, such as base shear, maximum distortion, or ductility demand.

4. Multi-Degree-of-Freedom PTSF Models

Five regular PTSF with semirigid connections designed according to the requirements of Mexico City Building Code [24] are considered in this study. It is assumed that the buildings which are used as offices have 3 bays and the number of stories ranges from 4 to 14. Their dimensions are shown in Figure 3(a), and in Figure 3(b) a detail of the posttension strands and the steel angles which represent the energy dissipating elements is shown. A36 steel and W sections are used in beams and columns. The assumed damping is 3% of the critical damping. The relevant characteristics of each frame, such as T_1, the shear force and the yield displacement (F_y and D_y), and the plastic stiffness of the main system with connections ($k_p = k_{\text{str}(p)} + k_{c(p)}$) are shown in Table 2. It can be observed that the structural frames present an ample interval of vibration periods ($0.89\,\text{s} < T_1 < 2.10\,\text{s}$). In the last two columns of Table 2, values of the postyielding and the initial stiffness of the structural system are given ($k_{\text{str}}, k_{\text{str}(p)}$).

5. Seismic Records

The structural models mentioned above are subjected to the action of several narrowband long duration earthquakes. Narrowband seismic motions have the special characteristic of considerably affecting specific structures in a short interval of periods, especially to structures that undergo "softening" [25, 26] or to structures with vibration periods close to the period of the ground. This type of records demands large amounts of energy to structures, compared to that demanded by broadband motions [2]. A set of 30 seismic motions recorded on soft ground of Mexico City are used in this study. The interval of magnitudes of the events goes from 6.9 to 8.1 (including the record obtained in the station "Secretaría de Comunicaciones y Transportes" (SCT) on September 19, 1985). The final seismic motions were obtained by rotating both horizontal components of the ground motion recorded in the station and maximizing their Arias intensity [27]. Details of the records are described in Table 3, where the last two columns represent the maximum acceleration and maximum velocity of the ground motion, respectively.

6. Transformation Factors of Hysteretic Energy

Transformation factors of hysteretic energy (FM_{EH}) according to (7) are presented in this section. Each of the frames described in Section 2 is analyzed under the action of the 30 accelerograms listed in Table 3. The ground motions are scaled in terms of the pseudoacceleration corresponding to the fundamental period of the frame ($S_a(T_1)$); the scaling ranges from 0.1 g to 1.7 g with increments of 0.1 g (where g is the gravity acceleration), in such a way that 510 records for each frame are obtained (a total of 2550 records for the 5 frames). A "step-by-step" nonlinear dynamic analysis in time domain is performed by using the RUAUMOKO computer program [28], and the response parameters in terms of moment rotation are obtained. The corresponding E_H is obtained by calculating the area enclosed by the hysteretic curve corresponding to each connection. For the analysis, it is assumed that the elements in each story dissipate equal amount of energy.

Figures 4(a), 4(b), 4(c), 4(d), and 4(e) show transformation factors for frames F4, F6, F8, F10, and F14, respectively.

Table 2: Dynamic characteristics of the steel frames with PTED.

Frame	Number of stories	T_1 (s)	F_y (kN)	D_y (m)	$k_{(p)}$ (kN/m)	k_{str} (kN/m)	$k_{str(p)}$ (kN/m)
F4	4	0.89	1030	0.050	2382	3270	501
F6	6	1.03	1570	0.072	2698	3250	658
F8	8	1.25	1570	0.072	2698	3656	654
F10	10	1.37	1766	0.082	2747	2600	545
F14	14	2.10	1373	0.100	1756	1308	147

Table 3: Characteristics of the accelerograms used.

Records	Date	Magnitude	Station	A_{ms} (m/s^2)	V_{ms} (m/s^2)
1	19/09/1985	8.1	SCT	1.780	0.595
2	21/09/1985	7.6	Tlahuac deportivo	0.487	0.146
3	25/04/1989	6.9	Alameda	0.450	0.156
4	25/04/1989	6.9	Garibaldi	0.680	0.215
5	25/04/1989	6.9	SCT	0.449	0.128
6	25/04/1989	6.9	Sector Popular	0.451	0.153
7	25/04/1989	6.9	Tlatelolco TL08	0.529	0.173
8	25/04/1989	6.9	Tlatelolco TL55	0.495	0.173
9	14/09/1995	7.3	Alameda	0.393	0.122
10	14/09/1995	7.3	Garibaldi	0.391	0.106
11	14/09/1995	7.3	Liconsa	0.301	0.096
12	14/09/1995	7.3	Plutarco Elías Calles	0.335	0.094
13	14/09/1995	7.3	Sector Popular	0.343	0.125
14	14/09/1995	7.3	Tlatelolco TL08	0.275	0.078
15	14/09/1995	7.3	Tlatelolco TL55	0.272	0.074
16	09/10/1995	7.5	Cibeles	0.144	0.046
17	09/10/1995	7.5	CU Juárez	0.158	0.051
18	09/10/1995	7.5	Centro urbano Presidente Juárez	0.157	0.048
19	09/10/1995	7.5	Córdoba	0.249	0.086
20	09/10/1995	7.5	Liverpool	0.176	0.063
21	09/10/1995	7.5	Plutarco Elías Calles	0.192	0.079
22	09/10/1995	7.5	Sector Popular	0.137	0.053
23	09/10/1995	7.5	Valle Gómez	0.179	0.0718
24	11/01/1997	6.9	CU Juárez	0.162	0.0590
25	11/01/1997	6.9	Centro urbano Presidente Juárez	0.163	0.0550
26	11/01/1997	6.9	García Campillo	0.187	0.0690
27	11/01/1997	6.9	Plutarco Elías Calles	0.222	0.0860
28	11/01/1997	6.9	Est. # 10 Roma A	0.210	0.0776
29	11/01/1997	6.9	Est. # 11 Roma B	0.204	0.0710
30	11/01/1997	6.9	Tlatelolco TL08	0.160	0.0720

It is important to note that for the first values of $S_a(T_1)$, there are no results of transformation factors because there is no dissipated energy E_H; on the other side, some graphs are truncated for big values of $S_a(T_1)$ because they correspond to structural failure. For example, Figure 4(a) shows that frame F4 failed for four ground motions (Ea17, Ea18, Ea19, and Ea21) before reaching the maximum intensity of 1.0 g. From Figures 4(a)–4(e), the following observations can be made: (1) the magnitude of FM_{EH} depends on the seismic intensity $S_a(T_1)$, when $S_a(T_1)$ increases, so does FM_{EH} and (2) the dispersion increases as $S_a(T_1)$ increases.

Figures 4(a)–4(e) also show that the mean value of FM_{EH} (μFM_{EH}), indicated by a black circles, can be reasonably fitted with a linear equation. The $FM_{EH}{}^*$ parameter is used for that purpose which is expressed by the equation

$$FM_{EH}{}^* = bS_a + c, \tag{8a}$$

where S_a is given as a fraction of the gravity acceleration and b and c are fitted in terms of the fundamental period of the frame under consideration, with the following equations:

$$b = -2.736T_1 + 9.169, \tag{9a}$$

$$c = 1.122T_1 - 4.230. \tag{9b}$$

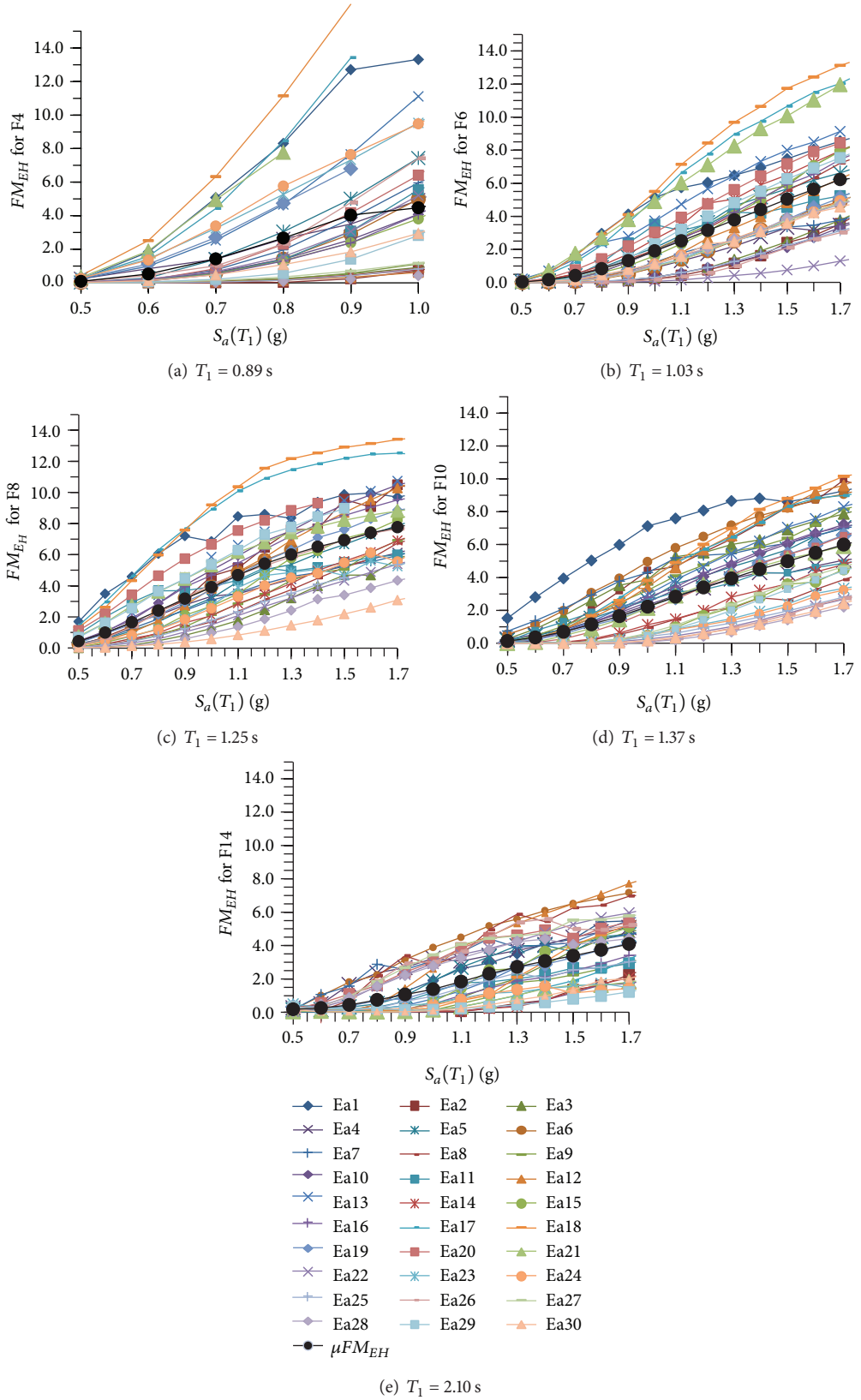

Figure 4: Transformation factors of E_H of frames F4 to F14.

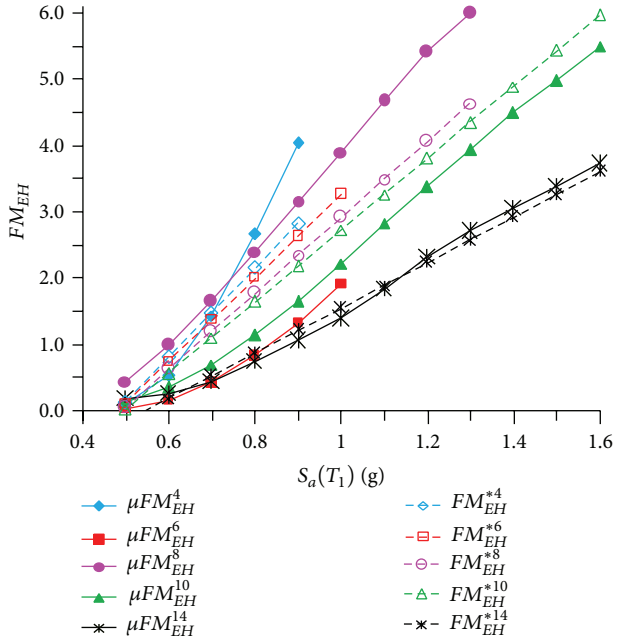

FIGURE 5: FM_{EH} in the ESDOFS.

Figure 5 shows with continuous lines the graphs of the mean values of FM_{EH} obtained from the results of the dynamic analyses and with dotted lines the $FM_{EH}{}^*$ values calculated with (8a), for all the structural models. It can be observed that the fitting obtained with (8a) is adequate.

7. Maximum Story Drift for the MDOFS

The maximum story drift (γ) is one of the main parameters used in the design codes to measure the damage and the performance of buildings under seismic actions; it is therefore useful to propose a simple procedure to determine the maximum story drift of posttensioned frames as a function of its fundamental structural period and of the seismic intensity. Figure 6 shows with continuous line the mean values of maximum drifts of F4, F6, F8, F10, and F14 for different intensity values of $S_a(T_1)$. It is observed that, except for frame F4, there is practically a linear variation of γ with $S_a(T_1)$. Using a regression analysis, the following equation to calculate γ is proposed:

$$\gamma^* = S_a\left(0.102e^{-1.245T_1}\right) + 0.005T_1 - 0.006, \qquad (10)$$

where γ^* is the maximum story drift, fitted to the mean values and expressed in radians.

Figure 6 shows with dotted lines the values of γ^* (obtained with (10)) for each of the frames studied and with continuous lines the values obtained from dynamic analyses. A good approximation is observed in all cases, although it is better for the frames with longer periods (greater height); the reason for this is that frames with lower height present nonlinear behavior for lower seismic intensities due to the structural "softening" phenomenon.

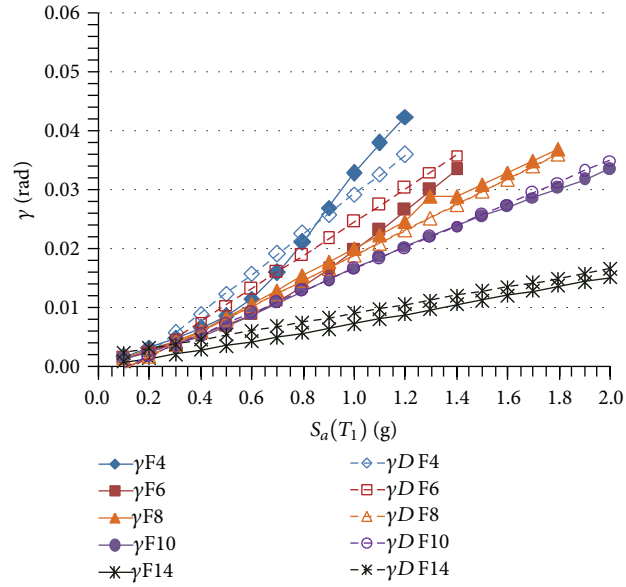

FIGURE 6: Maximum drift calculated for the MDOFS with PTDE.

8. Participation of the Connections in the Total Energy Dissipation (E_H)

As previously mentioned, the PTED are designed to dissipate most of the E_H. When the columns of the base are fixed at the foundation, plastic hinges are formed and some amount of E_H is dissipated. A similar situation may happen in other locations of the structure when the seismic demands increase considerably. Table 4 shows the factors of relative participation of the connections in the dissipation of the total E_H for the PTDE studied herein, calculated for different distortion demands. It is observed from the table that as the number of levels increases (thus increasing the number of connections) the participation of the energy dissipated by the connections also increases.

Table 4 also shows that taller frames (F10, F14) dissipate more energy (because they have more stories implying a large number of connections) than the smaller frames (F4). To calculate the relative participation of the dissipated energy of PTDE connections, (11a) is proposed, which is a function of the interstory drift demand γ (listed in the first column of Table 4). Coefficients q and r are calculated with (11b) and (11c) and both depend on T_1. The parameters were obtained through a regression analysis of the data presented in Table 4:

$$\text{FPC} = q\gamma + r, \qquad (11a)$$

$$q = -36.93T_12 + 55.47T_1 - 20.43, \qquad (11b)$$

$$r = 1.453T_1 - 1.018. \qquad (11c)$$

Figure 7 shows with continuous lines the values of the factors of participation of connections (FPC) obtained by means of the dynamic analysis of the PTDE and with dotted lines those calculated with (11a); a good approximation is observed for all frames. It is important to highlight that the

Table 4: E_H dissipated by the connections with respect to the total E_H.

γ	F4	F6	F8	F10	F14
0.015	0.287	0.444	0.630	0.806	0.982
0.020	0.278	0.424	0.564	0.720	0.929
0.030	0.272	0.398	0.492	0.596	—
0.050	0.273	0.356	—	—	—

PTSF studied herein are fixed at their base, which makes an important contribution to the base columns in the total dissipated energy E_H. In the case of columns with hinged bases, the participation is null.

9. Distribution of the Dissipated Energy through the Height of the Structure

It is known that the demands of E_H are not uniformly distributed in the structure; moreover, one of the main objectives in the design of PTSF with dissipating elements is that the E_H is dissipated at the connections, while beams and columns remain essentially elastic [29–31]. As previously mentioned, this is true except when the columns are fixed at the base; in this case, even for moderate seismic demands, plastic hinges are formed in the base, dissipating important amounts of E_H.

After calculating the total E_H in the ESDOFS, as shown previously, it is necessary to determine how the E_H is distributed through the height of the structure. Considering that the connections with PTED devices in each story dissipate equal amount of energy, López-Barraza et al. [32] proposed (12a) to calculate distribution factors of E_H (F_{EHi}). To obtain the energy dissipated in each story, the factors should be multiplied by the energy (E_H) dissipated by the connections:

$$F_{EHi} = \frac{1}{f_1(\gamma)(h_i/H)} \exp\left\{-\frac{1}{2}\left[\frac{\ln(h_i/H) - \ln(f_2(\gamma))}{f_3(\gamma)}\right]\right\}, \quad (12a)$$

$$f_1(\gamma) = 5.343\gamma + 2.433, \quad (12b)$$

$$f_2(\gamma) = 1.380\gamma + 0.388, \quad (12c)$$

$$f_3(\gamma) = 8.374\gamma + 3.316, \quad (12d)$$

where H is the total height and h_i is the height of the ith story measured from the base; the functions f_1,f_2, and f_3, given by (12b), (12c), and (12d), respectively, are obtained by using regression analysis.

10. Calculation of the Energy Dissipated in PTSF Based on the Results of ESDOFS

Using the mathematical expressions proposed in this study, an algorithm to find the distribution of the hysteretic energy dissipated through the height of the PTSF is presented in the following.

(1) Calculate the total E_H by using ESDOFS.

(2) Calculate the transformation factors $FM_{EH}{}^*$, substituting $S_a = S_a(T_1)$ in (8a).

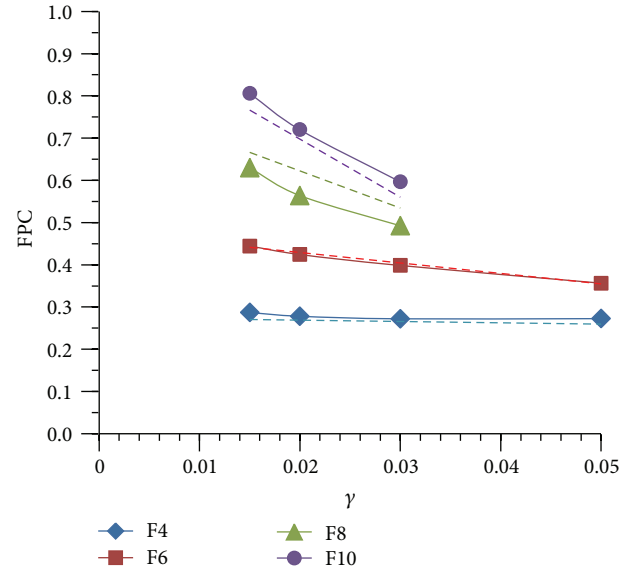

Figure 7: FPC as function of the drift.

(3) Calculate the total E_H of the PTSF.

(4) Calculate the interstory drift value (γ) with (10), corresponding to $S_a(T_1)$ and T_1.

(5) Calculate the relative participation of the connections (FPC), substituting γ in (11a).

(6) Calculate the energy dissipated by the connections.

(7) Calculate the energy distribution factors F_{EHi} corresponding to the ith story of the PTSF, substituting γ in (12a).

(8) Calculate the demand of E_H in the ith story (E_{HCi}).

It is important to note that the difference between E_{MDOFS} and E_{HC} is the hysteretic energy that the base columns dissipate when they are fixed.

11. Conclusions

(i) The study proposes a methodology to estimate the hysteretic energy (E_H) dissipated through the height of regular posttensioned steel frames with energy dissipating elements, based on the E_H dissipated by equivalent single-degree-of-freedom systems (ESDOFS) and by some simple mathematical expressions proposed here. These relate (1) the interstory drifts of the PTSF with the seismic intensity and the fundamental structural vibration period

(10), (2) the relative participation of the connections with respect to the total dissipated energy (11a), (11b), and (11c), and (3) the distribution of the dissipated energy as a function of the interstory drift (12a), (12b), (12c), and (12d).

(ii) The expressions are simple and can be applied to fixed PTSF with dissipating elements, with fundamental structural vibration periods ranging between 0.89 and 2.1s, located in soft soils of the valley of Mexico; however, the general methodology proposed here is applicable to PTSF with different structural conditions.

(iii) Furthermore, spectra of E_H to be included in the methods of seismic design can be developed. It is observed that for frames with few connections, such as F4, the efficiency in the dissipation of E_H is small due to the reduced number of PTED connections. For this case, other energy dissipating mechanisms may be considered.

(iv) The methodology and the expressions proposed here are useful tools for the seismic design or structural revision of PTSF with energy dissipating elements. For this purpose, it would be necessary to verify that the energy dissipating structural capacity is larger or equal to the energy demand. In addition, it would be also necessary to verify the requirements related to ductility capacity and maximum interstory drifts.

Conflict of Interests

The authors declare that there is no conflict of interests regarding the publication of this paper.

Acknowledgments

The support given by PROMEP under Grant UAS-PTC-060 and the Universidad Autónoma de Sinaloa under Grant PROFAPI2013/160 is appreciated. Financial support also was received from the Universidad Nacional Autónoma de México under Project PAPIIT-IN102114.

References

[1] C. M. Uang and V. V. Bertero, "Evaluation of seismic energy in structures," *Earthquake Engineering & Structural Dynamics*, vol. 19, no. 1, pp. 77–90, 1990.

[2] A. Teran-Gilmore, "Energy concepts and damage indices," in *Proceedings of the Symposium CUREe-EERC*, Report no. UBC/EERC-97/05, pp. 133–140, 1997.

[3] A. Terán-Gilmore and J. O. Jirsa, "Energy demands for seismic design against low-cycle fatigue," *Earthquake Engineering and Structural Dynamics*, vol. 36, no. 3, pp. 383–404, 2007.

[4] E. Bojórquez and S. E. Ruiz, "Strength reduction factors for the valley of Mexico taking into account low cycle fatigue effects," in *Proceedings of the 13th World Conference on Earthquake Engineering*, Paper 516, Vancouver, Canada, 2004.

[5] G. W. Housner, "Limit design of structures to resist earthquakes," in *Proceedings of the 1st World Conference on Earthquake Engineering*, Berkeley, Calif, USA, 1956.

[6] H. Akiyama, *Earthquake-Resistant Limit-State Design for Buildings*, University of Tokyo Press, Tokyo, Japan, 1985.

[7] B. Akbas, J. Shen, and H. Hao, "Energy approach in performance-based seismic design of steel moment resisting frames for basic safety objective," *The Structural Design of Tall Buildings*, vol. 10, no. 3, pp. 193–217, 2001.

[8] H. Choi and J. Kim, "Energy-based seismic design of buckling-restrained braced frames using hysteretic energy spectrum," *Engineering Structures*, vol. 28, no. 2, pp. 304–311, 2006.

[9] E. Bojorquez, S. E. Ruiz, and A. Terán Gilmore, "Reliability-based evaluation of steel structures using energy concepts," *Engineering Structures*, vol. 30, no. 6, pp. 1745–1759, 2008.

[10] C. Christopoulos, A. Filiatrault, and C. M. Uang, "Self-centering post-tensioned energy dissipating (PTED) steel frames for seismic regions," Tech. Rep. SSRP-2002/06, University of California, San Diego, Calif, USA, 2002.

[11] M. M. Garlock, R. Sause, and J. Ricles, "Design and behavior of post-tensioned steel moment frames," in *Proceedings of the 13th World Conference on Earthquake Engineering*, Paper 2560, Vancouver, Canada, August 2004.

[12] M. Wolski, J. M. Ricles, and R. Sause, "Seismic resistant self-centering steel moment resisting frames with bottom flange friction devices," in *Proceedings of the 5th International Conference on the Behavior of Steel Structures in Seismic Areas (STESSA '06)*, pp. 481–487, Yokohama, Japan, August 2006.

[13] K.-C. Tsai, C.-C. Chou, C.-L. Lin, P.-C. Chen, and S.-J. Jhang, "Seismic self-centering steel beam-to-column moment connections using bolted friction devices," *Earthquake Engineering and Structural Dynamics*, vol. 37, no. 4, pp. 627–645, 2008.

[14] C.-C. Chou and J.-H. Chen, "Column restraint in post-tensioned self-centering moment frames," *Earthquake Engineering and Structural Dynamics*, vol. 39, no. 7, pp. 751–774, 2010.

[15] C.-C. Chou and J.-H. Chen, "Seismic design and shake table tests of a steel post-tensioned self-centering moment frame with a slab accommodating frame expansion," *Earthquake Engineering and Structural Dynamics*, vol. 40, no. 11, pp. 1241–1261, 2011.

[16] A. López-Barraza, E. Bojórquez, S. E. Ruiz, and A. Reyes-Salazar, "Reduction of maximum and residual drifts on posttensioned steel frames with semi-rigid connections," *Advances in Materials Science and Engineering*, vol. 2013, Article ID 192484, 11 pages, 2013.

[17] Y. K. Wen, "Method for random vibration of hysteretic systems," *Journal of the Engineering Mechanics Division, ASCE*, vol. 102, no. 2, pp. 249–263, 1976.

[18] R. M. Richard and B. J. Abbott, "Versatile elastic plastic stress-strain formula," *ASCE Journal of Engineering Mechanics*, vol. 101, no. 4, pp. 511–515, 1975.

[19] A. López-Barraza, S. E. Ruiz, A. Reyes-Salazar, and E. Bojórquez, "Hysteretic model of steel connections for self-centering frames based on experimental studies of angles," in *Proceedings of the World Congress on Advances in Structural Engineering and Mechanics (ASEM '13)*, Jeju, Republic of Korea, September 2013.

[20] R. Bouc, "Forced vibration of mechanical system with hysteresis," in *Proceedings of the 4th International Conference Nonlinear Oscillations*, Praha, Czech Republic, 1967.

[21] T. T. Baber and Y. K. Wen, "Random vibration of hysteretic, degrading systems," *Journal of the Engineering Mechanics Division, ASCE*, vol. 107, no. 6, pp. 1069–1087, 1981.

[22] F. Casciati and L. Faravelli, *Fragility Analysis of Complex Structural Systems*, John Wiley & Sons, 1991.

[23] N. Shome and C. A. Cornell, "Simulation of non-stationary random process," *Journal of Engineering Mechanics, ASCE*, vol. 93, pp. 11–40, 1998.

[24] RCDF, Reglamento de Construcciones para el Distrito Federal, 2004.

[25] M. A. Montiel and S. E. Ruiz, "Influence of structural capacity uncertainty on seismic reliability of buildings under narrow-band motions," *Earthquake Engineering and Structural Dynamics*, vol. 36, no. 13, pp. 1915–1934, 2007.

[26] S. E. Ruiz, M. A. Montiel, and M. Arroyo, "Probabilities of exceeding different limit states for buildings subjected to narrow-band ground motions," *Earthquake Spectra*, vol. 26, no. 3, pp. 825–840, 2010.

[27] C. Villa-Velázquez, *Análisis de movimientos sísmicos registrados en el valle de México [Undergraduate. thesis]*, Universidad Nacional Autónoma de México (UNAM), 2001.

[28] A. Carr, *RUAUMOKO Inelastic Dynamic Analysis Program*, University of Canterbury, Department of Civil Engineering, 2011.

[29] J. M. Ricles, R. Sause, M. M. Garlock, and C. Zhao, "Posttensioned seismic-resistant connections for steel frames," *ASCE Journal of Structural Engineering*, vol. 127, no. 2, pp. 113–121, 2001.

[30] M. Garlock, R. Sause, and J. Ricles, "Design and behavior of post-tensioned Steel moment frames," in *Proceedings of the 13th World Conference on Earthquake Engineering*, Paper 2560, Vancouver, Canada, 2004.

[31] C. Christopoulos, A. Filiatrault, and B. Folz, "Seismic response of self-centring hysteretic SDOF systems," *Earthquake Engineering and Structural Dynamics*, vol. 31, no. 5, pp. 1131–1150, 2002.

[32] A. López-Barraza, S. E. Ruiz, A. Reyes-Salazar, and E. Bojórquez, "Seismic energy demands on steel framed structures with rigid and, alternatively, with post-tensioned semi-rigid connections," in *Proceedings of the 7th Conference Behavior of Steel Structures in Seismic Areas (STESSA '12)*, Santiago, Chile, 2012.